Eur Biophys J (1988) 15: 257–268

European Biophysics Journal

Review

Low resolution structures of biological complexes studied by neutron scattering

P. A. Timmins* and G. Zaccai

Institut Laue-Langevin, 156X, F-38042 Grenoble, France

Received March 25, 1987

Key words: Contrast variation, nucleoproteins, ribosomes, viruses, membrane structure.

Neutron scattering has been an established technique in solid state physics for some 30 years and in the last 10 years has had a significant impact in biological structure determination. This is especially true in the field of low to medium resolution structure, where complementary techniques are electron microscopy, X-ray scattering and the more indirect biophysical techniques such as hydrodynamic measurements. Small angle neutron scattering from solutions of particles and diffraction from ordered or partially ordered arrays of particles have made it possible to examine the distribution of different components of a *biomolecular complex in-situ* by substituting D_2O for H_2O in the molecular environment and/or D for H in the complex. Such investigations cannot be performed with other techniques. Several reviews on applications of neutron scattering have been published in the last few years [e.g. 1, 2, 3].

Method

Contrast

An object may only be visualized through a scattering experiment when its scattering density is different from that of its environment. This concept is in fact very familiar in both light microscopy and electron microscopy where *staining* of specimens is a standard technique. In scattering experiments, the particle may be either in solution (disordered) or in a hydrated ordered system such as a crystal, membrane or fibre.

For the purposes of low resolution scattering we consider the solvent to be a homogeneous continuum of scattering density ϱ^0. The contrast between a volume of scattering density ϱ and the solvent is defined as $\varrho - \varrho^0$.

It is clear that $\varrho - \varrho^0$ can be varied by changing either ϱ or ϱ^0 – the equivalents of + *ve* and – *ve* staining respectively in electron microscopy. The way to do this for neutron scattering depends almost entirely on the difference in scattering power between natural hydrogen (predominantly ^1H) and its heavier isotope ^2H (D, deuterium). The scattering density of H_2O is -0.00562×10^{-12} cm/Å^3 whilst that of D_2O is 0.064×10^{-12} cm/Å^3 and H_2O/D_2O mixtures are a linear combination of these values. Note that at 8% D_2O, $\varrho^0 = 0$; an experiment in these conditions would visualise the particle as if it were in a vacuum. The scattering density of a biological macromolecule is not a constant but also a linear function of the deuterium content of its aqueous environment because of the exchange of its labile hydrogen atoms with those of the solvent. The variation of mean values of ϱ for biological molecules and ϱ^0 for H_2O/D_2O mixtures is plotted as a function of percentage of D_2O in the solvent in Fig. 1. This also shows the scattering density of molecules where covalently bound protons have been exchanged for deuterium. It also shows the "match" points or "isopicnic" points of different components. These are solvent compositions which match the mean scattering density of the component. At these points the contribution of a component to the scattering is minimised. Changing the contrast by varying ϱ^0 is straightforward – it requires simply that a solution of particles be exhaustively dialysed against an appropriate D_2O/H_2O mixture. Contrast variation by changing ϱ, the scattering density of the particle, can be carried out by chemical labelling, and/or by *in vivo* deuteration such that the non-labile hydrogen atoms of a molecule are replaced by deuterium through biosynthetic incorporation.

* To whom offprint requests should be sent

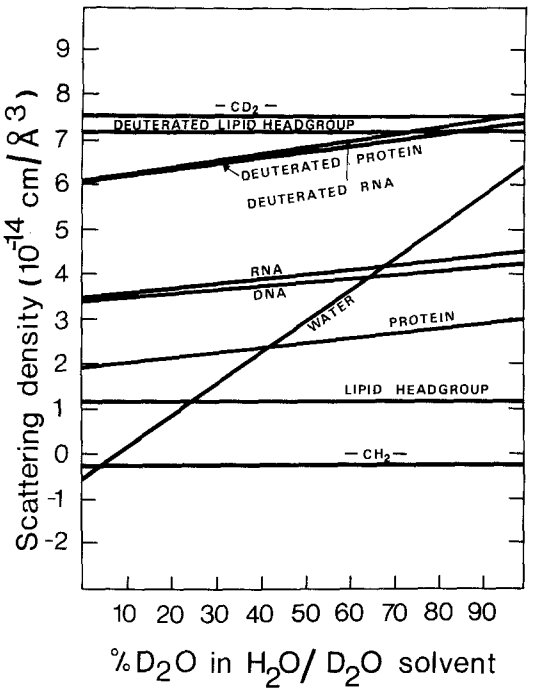

Fig. 1. Scattering density of different chemical components of biological complexes as a function of the D_2O/H_2O mixture in which they are immersed. The scattering densities are calculated assuming that all labile hydrogens (e.g. those attached to O or N) do in fact exchange with the solvent except in proteins where a figure of 80% exchange is assumed. Horizontal lines (e.g. $-CH_2-$) are for compounds having no labile hydrogen

Scattering and contrast

As the scattering density of both particle and solvent must be linearly dependent on the deuterium content of the solvent the contrast in a solvent containing a mole fraction X of D_2O can be written:

$$\varrho - \varrho^0 = (\varrho - \varrho^0)_{H_2O} + X(\varrho - \varrho^0)_{HD}, \quad \text{(i)}$$

where the subscript H_2O refers to the structure in H_2O and HD to the scattering density increment on going from H_2O to D_2O.

The wave scattered by a particle dissolved in solvent ϱ^0 is described by

$$\boldsymbol{F}(\boldsymbol{Q}) = \sum_j [(\varrho(\boldsymbol{r}_j) - \varrho^0)\, v_j \exp i\, \boldsymbol{Q}\boldsymbol{r}_j] = \boldsymbol{F}_{H_2O}(\boldsymbol{Q}) + X\boldsymbol{F}_{HD}(\boldsymbol{Q}), \quad \text{(ii)}$$

where $\boldsymbol{F}$ is a vector quantity describing the amplitude and phase of the scattered wave (the structure factor) at point $\boldsymbol{Q}$ ($Q = 4\pi \sin\theta/\lambda$; 2θ = scattering angle, λ = wavelength) in reciprocal space, from a particle of excess scattering density $\varrho(\boldsymbol{r}_j) - \varrho^0$ at point $\boldsymbol{r}_j$ with associated volume v_j. The observed intensity of this scattered wave depends on whether the particles are arranged in a crystal (or partly ordered system) or in solution.

In the *crystal* case the scattered intensity is given by the square of the structure factor amplitude (5, 6).

$$I(\boldsymbol{Q}) = |F(\boldsymbol{Q})|^2 = |\boldsymbol{F}_{H_2O}(\boldsymbol{Q})|^2 + 2X|\boldsymbol{F}_{H_2O}(\boldsymbol{Q})|\,|\boldsymbol{F}_{HD}(\boldsymbol{Q})|\cos\phi + X^2|\boldsymbol{F}_{HD}(\boldsymbol{Q})|^2. \quad \text{(iii)}$$

As there is constructive interference, $I(\boldsymbol{Q})$ is zero at all points except for $\boldsymbol{Q}$ = reciprocal lattice vector. ϕ is the phase difference between $\boldsymbol{F}_{HD}$ and $\boldsymbol{F}_{H_2O}$. In the case of a centro-symmetrical structure where $\phi = 0$ or π then

$$I(\boldsymbol{Q}) = \{|\boldsymbol{F}_{H_2O}(\boldsymbol{Q})| + X|\boldsymbol{F}_{HD}(\boldsymbol{Q})|\}^2, \quad \text{(iv)}$$

i.e. the square root of the intensity is linear with contrast.

Thus the amplitude $|F(\boldsymbol{Q})|$ may be measured or calculated for any contrast and if the corresponding phase can be determined then the scattering length density at any point in the particle can be computed by the reverse Fourier transform of Eq. (ii).

In the infinitely dilute *solution* case where there are no inter-particle interactions or preferential orientations and the solution is monodisperse, i.e. contains only one particle type, the measured intensity $I(\boldsymbol{Q}) = \langle|\boldsymbol{F}(\boldsymbol{Q})|^2\rangle$ where $\langle\,\rangle$ denotes an average over all possible orientations of the particle. The scattering is therefore isotropic and $\boldsymbol{Q}$ becomes a scalar quantity

$$I(\boldsymbol{Q}) = \langle|\boldsymbol{F}_{H_2O}(\boldsymbol{Q})|^2 + 2X\cos\phi\,|\boldsymbol{F}_{H_2O}(\boldsymbol{Q})|\,|\boldsymbol{F}_{HD}(\boldsymbol{Q})| + X^2|\boldsymbol{F}_{HD}(\boldsymbol{Q})|^2\rangle. \quad \text{(v)}$$

Thus again $I(\boldsymbol{Q})$ is a quadratic function of X.

For a detailed discussion of this interpretation of contrast variation the reader is referred to various reviews [1, 2, 3].

The averaging in (v) means that $\boldsymbol{F}(\boldsymbol{Q})$ cannot be determined directly (except in the special case of a spherical particle). However, at resolutions corresponding to the particle size:

$$I(\boldsymbol{Q}) \simeq I(0)\exp(-Q^2R_g^2/3) \quad \text{(vi)}$$

$$\text{i.e. } \ln I(\boldsymbol{Q}) \simeq \ln I(0) - \frac{Q^2R_g^2}{3}. \quad \text{(vii)}$$

This is the Guinier approximation which is valid in the range $QR_g \lesssim 1$. Hence from a plot of $\ln I(\boldsymbol{Q})$ v Q^2, $I(0)$ and R_g may be determined. For a monodisperse solution in the limit of infinite dilution, i.e. when all interactions between particles can be neglected, $I(O)$ and R_g^2 are related to the total excess scattering and to its distribution in the particle, respectively.

$$I(0) \propto F^2(0) = [\sum_j (\varrho(\boldsymbol{r}_j) - \varrho^0)\, v_j]^2 \quad \text{(viii)}$$

$$R_g^2 = \frac{\sum_j (\varrho(\boldsymbol{r}_j) - \varrho^0)\, v_j r_j^2}{\sum_j (\varrho(\boldsymbol{r}_j) - \varrho^0)\, v_j}, \quad \text{(ix)}$$

(where r_j is the distance from the centre of mass of $\varrho(r_j) - \varrho^0$). $I(0)$, the intensity at zero angle, is related to the molecular weight and R_g, the radius of gyration, to the shape. The analytical behaviour of $I(0)$ and R_g as a function of contrast has been described in detail by Ibel and Stuhrmann [4].

Both $I(O)$ and R_g^2 refer to the particle in solution and not necessarily to the macromolecule. The distinction is that the particle is defined as the volume not occupied by homogeneous solvent [3]. This volume includes the interactions and perturbations caused in the solvent by the presence of the macromolecule. A thermodynamic approach to the interpretation of $I(0)$ has been developed, which relates it to a scattering density increment, similar to the mass density increment used in the interpretation of analytical centrifugation results [87]. These density increments contain information on solvent-macromolecule interactions and such an analysis represents the most rigorous approach to the interpretation of $I(0)$. The relation between the particle and thermodynamic approach has been discussed in a review [3].

Beyond the Q region where the Guinier approximation is valid, $I(Q)$ can only be interpreted by comparing it to model calculated curves. Contrast variation is a very powerful technique for the approach. By suitably deuterating a complex sample it is possible to obtain a measured $I(Q)$ corresponding to a very simple structure by matching to the solvent all but a small part of the particle. In the triangulation method [9, 10], for example, the final $I(Q)$ corresponds in principle to the structure factor of two points separated by a fixed distance. By labelling different pairs of "points" in the complex, its structure can be modelled, distance by distance.

Applications

The usefulness of deuterium labelling and contrast variation derives from the different contrast behaviour of various components of a biological complex. It is, therefore, convenient to discuss applications of the technique in terms of the type of components forming the complex, e.g. proteins, nucleic acids, lipids ... etc. In addition, the contrast may be manipulated in such a way as to highlight interactions between macromolecule and solvent.

Protein-nucleic acid complexes

Protein-nucleic acid interactions form the basis of many of the most important recognition and control systems of the cell. The electron densities of protein and hydrated nucleic acid are similar so that X-rays or electron microscopy cannot easily distinguish between the two chemical components at low resolution. X-ray crystallography has been able to determine certain high resolution features of viruses [7] but in these cases inherent disorder has prevented even low resolution information from being obtained about a large part of the structure. Neutron scattering is particularly useful in this context owing to the large difference in scattering length densities between the nucleic acid and protein and the technique has been applied successfully to a large number of protein-nucleic acid complexes in solution as well as to single crystals.

The ribosome

Probably the most extensive neutron scattering studies carried out have been on the structure of the prokaryotic ribosome (results to 1979 are reviewed in [8]). The 70*S* ribosome of *E. Coli* is the site of protein synthesis. It can be dissociated into two subunits sedimenting at 30*S* and 50*S*. These particles contain, respectively, 21 and 32 different proteins, whilst the 30*S* contains one strand of RNA of MW $\sim 0.5 \times 10^6$ and the 50*S* subunit contains two RNA strands of $\sim 1.0 \times 10^6$ and $\sim 4 \times 10^4$. The determination of the quaternary structure of these particles is an enormous problem and one requiring the use of many techniques. In the early 1970's it was proposed that the distances between pairs of individual protein molecules in the ribosome could be measured by neutron scattering studies if pairs of specifically deuterated proteins could be incorporated into the ribosome [9, 10]. Thus was born the *label triangulation method.* The method has now been applied successfully to both the 30*S* and 50*S* subunits [11, 12]. Figure 2 shows

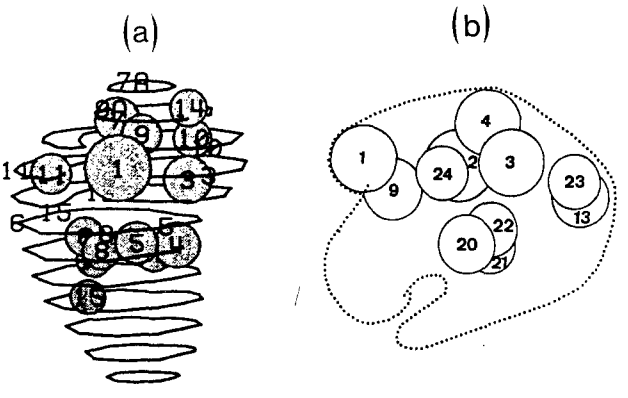

Fig. 2. a Superposition of the neutron map of the 30*S* ribosomal sub-unit on the electron microscopic image. The contours represent the outline of the sub-unit as seen by negative staining in the electron microscope. Circled numbers are neutron located proteins and uncircled numbers the positions of corresponding antigenic determinants as found by antibody staining (From [11]). **b** Positions of 11 of the 32 proteins in the 50*S* ribosomal subunit. The dotted line indicates the boundary of the particle derived from electron microscopy (R.P. May, V. Novotny, P. Novotny and K. Nierhaus, unpublished)

maps of the protein positions in the 30*S* and 50*S* subunits. These positions on the whole agree with and complement those found by immune electron microscopy. In this latter case the technique localises a specific antigenic determinant whereas the neutron measurement gives the position of the centre of mass of the protein.

An important adjunct to the measurement of inter-protein distances within the ribosome has been the determination of the shapes of these proteins, especially in view of suggestions that ribosomal proteins are often unusually elongated compared to normal globular proteins. The first method used was to measure the scattering from single isolated proteins in solution [13]. Contrast variation experiments on the complex between protein *S*4 (a constituent of the small subunit) and a 13*S* fragment of ribosomal RNA have also been carried out, allowing the radius of gyration of each constituent to be estimated at the match point of the other constituent [14], and showed the *in situ* radius of gyration of protein and RNA to be the same within error as that found for the free molecules.

Much recent work has been devoted to the measurement of *in situ* protein shapes in ribosomal subunits by specific deuteration [12]. In this method ribosomes are grown in various D_2O concentrations, dissociated and the components reassociated such that the average scattering length densities of the protein and RNA are the same whilst the one protein to be investigated is incorporated in its hydrogenated form. The scattering curve is then measured where the contrast of the RNA/protein matrix is a minimum. Of course, if this contrast were zero, the scattering curve would be that of the protein under study. Model calculations have been performed to analyse the contribution of the matrix to the scattering and show that such effects are negligeable in the Q-range used for measuring the scattering from individual proteins. This very elegant technique requires advanced biochemistry for dissociation and specific reconstitution. Most of the *in situ* radii of gyration measured tend to support the view that ribosomal proteins are compact.

The results of triangulation experiments on the 30*S* sub-unit [11] appeared to be in contradiction with early H_2O:D_2O contrast variation experiments [15, 16], which had been interpreted in terms of an RNA core surrounded by protein, both components having the same centre of mass. In a recent paper [17] the contrast variation experiments were found to be reproducible; however, it appeared that this type of preparation also contained non-ribosomal proteins. Salt-washing the subunits resulted in the removal of the non-ribosomal protein component and also of the protein *S*-1. Contrast variation experiments on the salt-washed subunits, were found to be more consistent with triangulation results, showing that protein and RNA are intermingled with a separation of 25 Å between their centres of mass. The latter result was derived from reconstituted subunits containing deuterated RNA and natural protein, as the natural contrast between RNA and protein was found to be insufficient for the measurement.

Amino-acyl tRNA synthetase interactions with tRNA

Amino-acyl tRNA synthetases are specific enzymes which catalyze the formation of amino-acyl tRNA. This interaction is essential to the process of recognition in which the correct amino-acid is incorporated in the nascent polypeptide chain. Solution scattering studies of the interactions have centred on the stoichiometry and structural change of the separate components by monitoring $I(0)$ and R_g as functions of contrast and tRNA-protein ratio. Such experiments involve a departure from the normal assumption of small angle scattering that we are considering a monodisperse solution of particles. Nevertheless, there are expressions for $I(0)$ and R_g for a mixture of different particles. The distribution of complexes can, therefore, be modelled by using association constants and the values of $I(0)$ and R_g. The analysis is simplified by contrast variation; the interactions being independent of H_2O:D_2O ratio in the buffer, the model for the particle distribution had to be compatible with contrasts where only protein contributed to $I(0)$ and R_g, and contrasts where tRNA also contributed. Thus protein-protein interactions were easily separated from tRNA-protein interactions. Results include a structural interpretation of anti-cooperativity in the methionyl-tRNA synthetase system of *E. Coli* [18], the observation of large conformational changes in the valyl, system from yeast [19], the measurement of the stoichiometry of tRNA binding in the aspartyl system from yeast (a value which was controversial from biochemical techniques) and defining crystallisation conditions for that enzyme/tRNA complex [20]. Results clarified for the first time the importance of protein-protein interactions in these systems.

A contrast variation study was also carried out on aspartyl tRNA synthetase-tRNA Asp crystals and has allowed the localisation of the enzyme molecule within this complex in the unit cell [21].

Nucleosome

The nucleosome core particle is the fundamental repeating unit of the chromosome. It consists of two copies each of four basic proteins called histones, complexed with approximately 146 base pairs of linear double-stranded DNA. The protein and DNA each

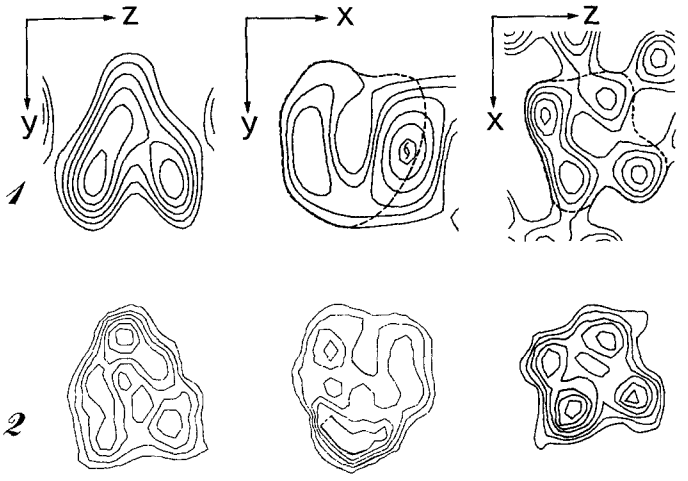

Fig. 3. Comparisons of (1) projections of the nucleosome core particle in 65% D_2O buffer, where only the protein is visualized and (2) orthogonal projections of the three-dimensional reconstruction of the histone octamers from electron micrographs of tubular aggregates. From [26]

comprise about 50% of the particle weight thus making it an ideal subject for a contrast variation study.

Neutron studies from solutions of core particles were the first to demonstrate unambiguously that the DNA is situated on the outside of a protein core [22, 23] and provided the overall dimensions of the particle. Experiments on nucleosomes and core particles at low ionic strength showed a structural transition related to unwinding of the ends of the DNA [24].

Nucleosome core particles were the first complexes to be studied successfully using contrast variation in single crystals [25–27]. This study allowed the parameters of the DNA superhelix to be determined and the shape of the protein core to be seen. Crystalline aggregates of the histone core had also been studied by electron microscopy and image reconstruction. Figure 3 shows projections of the structure obtained by electron microscopy from the protein and by neutrons from the nucleosome core particle in 65% D_2O where the DNA contribution to the scattering is a minimum. The remarkable similarity between them shows how the shape of the histone core is unaltered by taking off the DNA.

A recent controversy relating to the conformation of the histone octamer [28–30] may have been resolved by a neutron solution scattering experiment which demonstrated that salt conditions play an important role in determining its molecular shape [31]. In 2 *M* NaCl the octamer is shown to be similar in shape and size to the histone component of crystallized nucleosomes whereas in 3.5 *M* ammonium sulphate it is elongated in a manner similar to that observed in octamer crystals under the same conditions.

Viruses

Viruses consist of a protein coat enveloping a DNA or RNA genome which in simple viruses codes for the viral structural proteins and in more complex cases codes also for non-structural processing proteins. Some viruses contain also a lipid envelope which may or may not be derived from the host cell membrane.

Structural studies on viruses have been carried out particularly by electron microscopy. Some simple spherical plant viruses were amongst the first biological complexes crystallized over 50 years ago. X-ray crystallographic techniques however were not sufficiently sophisticated then and the atomic resolution structure of these viruses was not solved until the late 1970's. The structures of a number of spherical viruses are known; for example the plant viruses, Tomato Bushy Stunt Virus (TBSV) [7], Southern Bean Mosaic Virus (SBMV) [32] and Satellite Tobacco Necrosis Virus (STNV) [33] and the animal viruses, human rhinovirus 14 [34] and poliovirus [35]. Although the outer coat protein structure is well defined, in each case the RNA and varying amounts of the protein are invisible in electron density maps. In the larger spherical viruses the distribution of the various components, protein, lipid and nucleic acid is practically impossible to determine except by the contrast variation technique. The first application of the technique to the small spherical plant viruses showed the RNA and protein not seen by crystallography (Fig. 4). In TBSV there is a bilobal radial distribution of protein [36] and a more homogeneous distribution in SBMV [38].

The method has also been applied to the much larger animal viruses such as adenovirus [39] and influenza virus [40, 41]. In these cases the particles were originally less well characterised than the smaller plant viruses and such basic parameters as molecular weight were poorly known. Neutron scattering allowed the molecular weight of adenovirus to be determined as well as the radial distribution of DNA and protein (Fig. 4). In the case of influenza virus, a lipid-containing RNA virus, the molecular weight was redetermined and at the same time the chemical composition, in particular the protein/lipid ratio. The position of the lipid bilayer was also determined rather precisely. The model obtained is also shown in Fig. 4.

Recently the contrast variation method has been applied to single crystals of TBSV (P. A. Timmins, J. Witz, D. Wild; manuscript in preparation). Figure 5 shows the neutron scattering density in a section through the centre of the virus particle from a crystal soaked in 70% D_2O/H_2O. Under these conditions the RNA is essentially invisible and we see only the protein. It can therefore be seen that the protein is distributed in two shells, the outer capsid (whose structure has been determined by X-rays) and an inner, less well

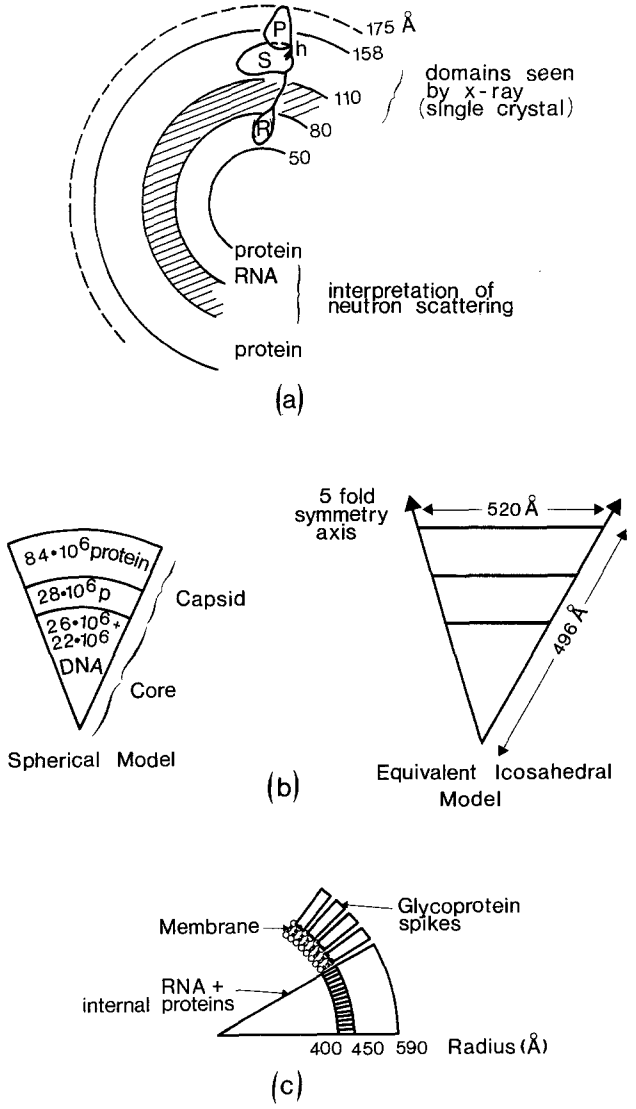

Fig. 4a–c. Information derived from small angle neutron scattering on spherical viruses. **a** *TBSV*: This shows how the neutron scattering studies complement the high resolution X-ray crystallography in identifying the radial location of the RNA and disordered protein. Reproduced from [37]. **b** *Adenovirus*: Dimensions of the nucleoprotein core and distribution of the protein in two shells of differing density. Reproduced from [39]. **c** *Influenza virus*: Showing the radial location of the lipid bilayer and the absolute amount of protein constituting the spikes. reproduced from [41]

ordered but nevertheless structured, shell. The two shells are connected by a vary tenuous density which probably represents an extended polypeptide chain.

Multisubunit protein complexes

The quaternary structure of multi-subunit proteins is accessible to study by neutron scattering only where subunits can be specifically deuterated. This has been

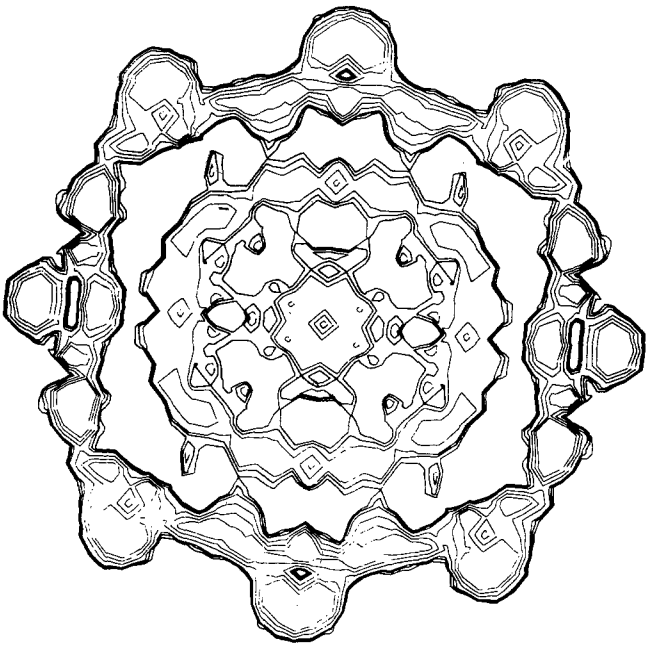

Fig. 5. The distribution of protein in tomato bushy stunt virus (TBSV) at 16 Å resolution. Section through the centre of the virus particle in 70% D_2O/H_2O where the RNA is contrast matched

successfully carried out for the DNA dependent RNA polymerase and for tryptophan synthase.

For the polymerase, an $\alpha_2\beta\beta'\sigma$ structure, distances between sub-units and sub-unit shapes *in situ* were determined from a label triangulation/contrast variation approach [42–44]. The same authors have recently developed a rational method for estimating the deuteration of the proteins as a function of the H_2O/D_2O content of the growth medium [45]. This is a general method which is applicable to all proteins isolated from *E. Coli*.

Tryptophan synthase is an $\alpha_2\beta_2$ multienzyme complex where deuterium labelling was used to measure the distance between the α sub-units as well as that between the two domains of each sub-unit [46]. The shape of the β_2 central sub-unit was also determined. These results have been confirmed recently by X-ray crystallography (C. C. Hyde, E. A. Padlan, S. A. Ahmed, E. W. Miles and D. R. Davies, personal communication).

Membranes and membrane components

Biological membranes are specialised structures with specific functional roles. They are made up primarily of lipids and proteins. Current thought regards the lipid as a support for the proteins, which are responsible for specific biological function. Lipid structure is nevertheless important in maintaining the permeabil-

ity barrier and allowing optimum protein function. Membranes are amphiphilic with hydrophilic faces on either side and a hydrophobic interior. It is generally accepted, although by no means established in all cases, that the lipids are in a bilayer, a structure similar to that of lamellar phases observed in pure lipid-water preparations [49–49]. In lipid characterisation nomenclature, $L\alpha$ phases are liquid crystalline with fluid, disordered acyl chains giving broad diffraction at a spacing of 4.5 Å; the $L\beta$ phases are gel-like with ordered, close-packed acyl chains giving sharp 4.2 Å diffraction. Diffraction from myelin, for example, is similar to that of $L\alpha$ [47]. Lipid fluidity is important in membranes such as retinal rod outer segment discs, where function requires the protein to diffuse in the membrane plane [50].

Until very recently the molecular structure of membrane proteins remained elusive. Studies were limited by crystallographic difficulties (at best one-dimensional order was achieved from membrane stacks [51]), and the complexity of membrane compositions. Extraction of membrane proteins to measure the most elementary structural information, such as sequence or molecular weight, for multi-subunit complexes, was very difficult because of the inadequacy of biochemical techniques to deal with their hydrophobic nature. Important break-throughs in membrane structure determination have been the discovery of naturally crystalline membrane systems such as purple membrane [52] and the development of detergents which allow extraction of active membrane proteins [53], and their crystallisation [54]. And in 1985, the first high resolution structure of an integral membrane protein was published [55].

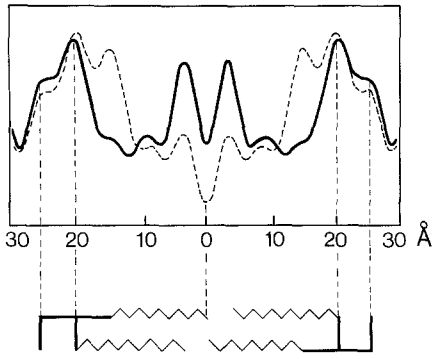

Fig. 6. Scattering density profile of a dipalmitoyl phosphatidyl choline (DPPC) lipid bilayer at low water content in the gel phase. The full line is with the $-CH_2-$ at positions 15 in the alkyl chains replaced by $-CD_2-$ and the dotted profile for similar labels in the C.5 positions. Below, the molecule is shown schematically with structural features which have been shown to be common to the liquid crystalline and gel phases: headgroup parallel to the plane of the membrane and non-equivalent chains

Lipid bilayers [56–60]

The time-averaged structure of lipid molecules in bilayer profiles has been described in great detail by neutron diffraction. The bilayer profile of a specifically deuterated lipid is shown in Fig. 6. Hydration of the headgroups was measured by H_2O:D_2O exchange. The conformations of the two different acyl chains as well as of the headgroup were established by specific chemical deuterium labelling (CD_2 groups replacing CH_2). Experiments were performed in the $L\alpha$ and $L\beta$ phases and for the two common headgroups of biological membranes: phosphatidyl choline and phosphatidyl ethanolamine. Specific labelling and contrast differences have also been used to describe the interaction of lipid water bilayers with cholesterol.

Purple membrane of H. Halobium

Purple membrane is naturally crystalline in two dimensions. The structure of bacteriorhodopsin, the only protein it contains, has been solved to 7 Å resolution by electron microscopy [52]. Its function as a light-activated proton pump has been studied extensively and it was the first membrane protein to be sequenced; the chromophore is one molecule of retinal bound to a lysine in the protein (reviewed in [61]). Considerable complementary structural information on this membrane has been obtained from neutron diffraction (summarised in Fig. 7). H_2O:D_2O exchange has shown that hydration is predominantly around lipid headgroups and that the protein does not have bulk water associated with it [62, 63]. This was an important result, excluding partial pores of bulk water in the proton pathway of the pump, or aqueous clefts either within a protein molecule or in between different protein molecules in the trimer. The hydration study was recently extended to liquid nitrogen temperatures [64], where the membrane structure is maintained but not its activity. The unit cell dimensions and hydration found for the different conditions indicated that bacteriorhodopsin in functional membranes (i.e. wet and close to room temperature) has a rather loosely-packed environment which would allow large amplitude, low frequency fluctuations of protein structure, that might be involved in its function. It is suggested to test this hypothesis by inelastic neutron scattering, which is a direct probe of protein dynamics [82, 83].

In a neutron diffraction approach to a higher resolution structure, based on the low resolution structure and the sequence, specific deuterated amino acids were incorporated in the structure by biosynthesis to act as labels [65]. Diffraction experiments on these samples suggested that the protein α-helices were embedded in the bilayer with their hydrophobic faces towards the

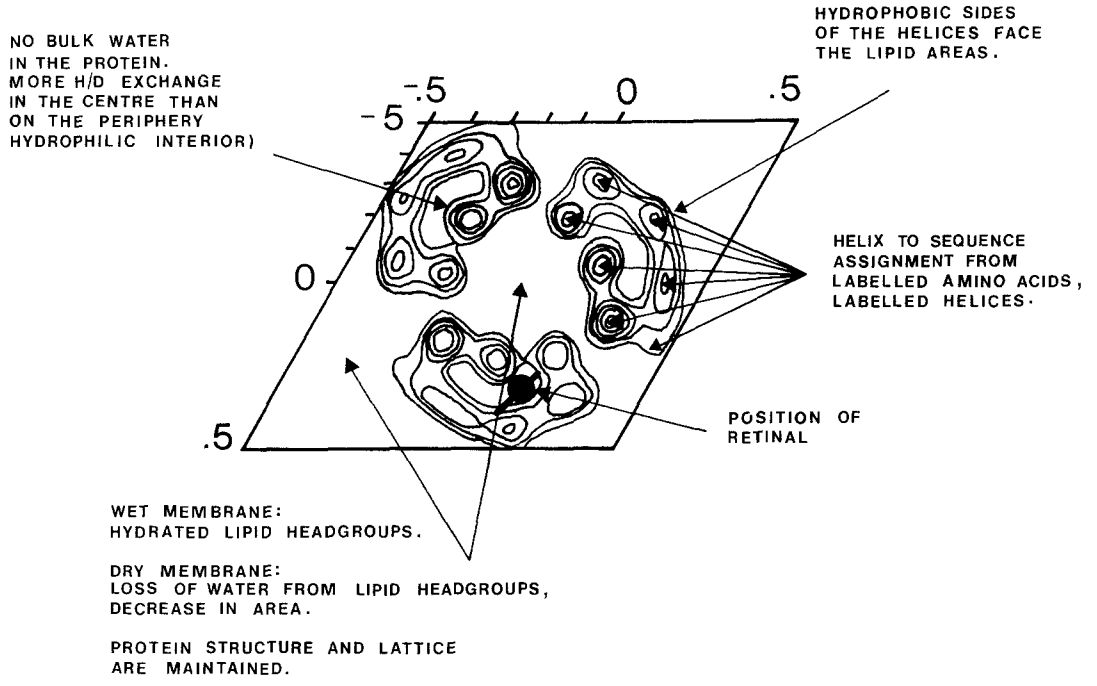

Fig. 7. A unit cell of purple membrane showing the information derived from neutron diffraction experiments. The contoured area represents three symmetry-related molecules each comprising seven alpha helices and the intervening space is filled with lipids

centre of the molecule away from the lipid. Sequence to helix assignments have also been suggested from these data [66]. In a more ambitious approach to solving the sequence-to-helix assignment problem, the bacteriorhodopsin lattice was reconstituted from denatured protein fragments [67] and studied by neutron diffraction by using natural and deuterated components [68]. In this way the first two sequence helices were located at one end of the structural projection of the molecule. The position and orientation of the retinal in the projection has been determined by using a sample where deuterated retinal was incorporated biosynthetically into the membrane [69, 70].

Solubilised membrane proteins and membrane protein crystals

To successfully separate the radii of gyration of two components of a complex by contrast variation it is not sufficient that the mean scattering density of one of the components match the solvent, it should also be homogeneous to the resolution required. This is particularly problematic in the case of lipids or detergents where the scattering density of the headgroup and hydrocarbon chain may be very different. The difficulty may, however, be overcome by partial deuteration and was achieved in a very detailed study of rhodopsin micelle complexes in which the radius of gyration of rhodopsin was measured and the geometry of its interaction with the detergent was determined [71].

The *in situ* molecular weight of membrane proteins is often a difficult parameter to determine, and the number of subunits in several membrane proteins remains unknown [72]. Provided a pure system can be solubilised in detergent or lipid, a small angle neutron scattering experiment with contrast variation provides a straightforward molecular weight determination of the system in the given conditions. If the radius of gyration is not required with precision, the other component (detergent, lipid) need not be homogeneous in scattering density. The method was applied successfully to the ATP/ADP transport protein solubilised in excess detergent [73].

Contrast variation is also applied in low resolution studies of membrane protein/detergent crystalline complexes. Matrix porin is a major component of *E. coli* outer membranes, and acts as a transmembrane channel allowing the passage of molecules of molecular weight up to 700. Preliminary neutron results from crystals of protein-detergent complexes show the protein trimer to be associated in such a way as to form three channels which exit on the periplasmic side of the membrane in a complicated fashion. The structure was solved by obtaining phases from model fitting [74] and then refining these by non-crystallographic symmetry averaging (Garavito, Timmins, Zulauf, private communication). The contrast variation approach was essential in distinguishing the protein from the detergent in which it is crystallized. Ambiguities do arise however at the junction between detergent and hydrophobic parts of the protein. These could be overcome by the use of deuterated detergent.

Solvent microenvironment of a macromolecule

The structure of a macromolecule in solution is determined in part by its interactions with solvent molecules, which in turn are perturbed by the macromolecule and may be structurally different from the bulk. A general model for a macromolecule in solution is a volume V_p containing the atoms of the macromolecule, a volume V' of perturbed solvent, and the whole surrounded by bulk solvent. The dissolved *particle* measured in a solution scattering experiment is not the macromolecule alone in V_p, but the entire volume of composition different from bulk solvent, i.e. $(V_p + V')$. The microenvironment, V', of a biological macromolecule could be very important in its functional interactions, yet there are very few experimental techniques available for its characterisation. Through the contrast variation approach, neutron scattering experiments from solution have been successful in separating the structure of a macromolecule from that of the perturbed solvent around it.

Transfer RNA, the case of polyelectrolytes

Charged macromolecules in solution have partial specific volumes which are functions of the salt composition of the solvent. This reflects volume differences in V' between the different conditions. Many cations, for example, have negative, partial specific volumes (electrostriction). It has been shown that, in an H_2O:D_2O contrast variation experiment, a volume of dense solvent can be observed around the tRNA [75, 76]; and its composition and radius of gyration were measured for different conditions. This was interpreted in terms of the Donnan equilibrium in which salt is excluded from the immediate vicinity of the macromolecule with an accumulation of positive counter ions. Electrostriction due to these counter ions also contributes to the effective high solvent density observed. The method of neutron contrast variation between tRNA and its immediate environment should be generally applicable to charged macromolecules.

Hydration and solvent interactions in proteins

A hydration shell around a macromelecule which excludes other small solutes can be measured directly by neutron small angle scattering if its contrast is different from that of the bulk solvent. In experiments on ribonuclease A, the hydration shell was investigated for glycerol and alcohol aqueous solvents [77]. Experiments were done in D_2O and the contrast was changed by varying the concentration of deuterated glycerol $C_3H_5(OD)_3$ and ethanol $C_2H_5(OD)$. This approach has the great advantage that there is no H-D exchange of labile H during the series of experiments. A hydration shell corresponding to 0.2 g of water per g of protein was observed to exclude glycerol but no hydration shell was observed in the alcohol case, i.e. the protein surface is equally accessible to alcohol and water, but 'repels' glycerol. The use of glycerol as a contrast variation agent for neutron solution scattering has been discussed quantitatively [78].

Halophilic enzymes are stable only in very high concentration of salt, and have solvent interactions (with both water and salt) that are more extensive than in non-halophilic proteins. A study of halophilic malate dehydrogenase has shown how neutron results can be combined with X-ray and ultracentrifugation data, in a generalized contrast variation approach, in order to determine separately structural and interaction parameters [79, 80]. Because, unlike X-rays or gravitational measurements, the neutron scattering length density of concentrated salt solvents is small compared to that of the protein, the use of the complementarity between these approaches is very powerful.

Conclusion

Low resolution neutron scattering has proved useful in many different kinds of problems. The neutron scattering density of a molecule is independent of its electron density, so that, in general, the neutron "view" is different from and complementary to that obtained by X-ray scattering. Experiments could be divided into broad classes:

(*1*) Complexes with high natural contrast between components (e.g. nucleoprotein).
(*2*) Complexes which can be specifically deuterated (e.g. ribosomes, multienzyme complexes).
(*3*) Salt-dependent conformation (e.g. histone octamer). Studies in high salt are difficult by X-rays because of low contrast.
(*4*) Interactions between solvent component and macromolecule (e.g. tRNA, halophilic enzymes).

In this review we have attempted to point out some of the major contributions of neutron scattering to the field of molecular biology. We have been highly selective in our choice of examples and many important contributions have not been mentioned as our aim was to give an illustrative rather than an exhaustive review. Neutrons have also been very useful, for example, for rapid measurements of molecular weight and radius of gyration of macromolecules in solution [81]. These most elementary parameters are often not known and are difficult to measure by other techniques. Neutron scattering with a very small amount of sample

(< 1 mg) in any buffer is a non-destructive technique which can provide a very rapid characterisation.

We have considered only the *structural* aspects of molecular biology, although inelastic neutron scattering is now taking its first steps into the investigation of the dynamics of biological macromolecules and their environment [83, 84]. The next few years should clarify the usefulness of neutrons in this domain.

We have also omitted mention of high resolution neutron crystallography which has also provided many exciting results [85].

The growth of neutron small angle scattering can be traced to both a combination of biochemical advances and progress in neutron technology – particularly the development of high flux reactors, cold neutron beams and multi-detectors. Further progress will most probably depend more on advanced biochemistry. Specific deuteration has still not been fully exploited, partly because of the important investment in sample preparation. Advances in genetic engineering should allow pure molecules and complexes to be produced in the milligram quantities necessary for direct structural techniques rather than the micrograms or nanograms used for many functional characterisations.

Neutron scattering is a non-destructive technique and also one which is amenable to many different kinds of sample environment through the possibility of having strong, transparent sample containers. We can therefore look forward to manipulations of thermodynamic parameters such as pressure or temperature [64, 86–88].

References

1. Engelman DM, Moore PB (1975) Determination of quaternary structure by small angle neutron scattering. Annu Rev Biophys Bioeng 4:219–239
2. Jacrot B (1976) The study of biological structures by neutron scattering from solution. Rep Prog Phys 39:911–953
3. Zaccai G, Jacrot B (1983) Small angle neutron scattering. Annu Rev Biophys Bioeng 12:139–157
4. Ibel K, Stuhrmann HB (1975) Comparison of neutron and X-ray scattering of dilute myoglobin solutions. J Mol Biol 93:255–265
5. Worcester DL (1976) Neutron diffraction studies of biological membranes and membrane components. In: Schoenborn BP (ed) Neutron scattering for the analysis of biological structures. Brookhaven Symp Biol N7:III-37–III-57
6. Hulmes DJS, Miller A, White SW, Timmins PA, Berthet-Colominas C (1980) Interpretation of the low-angle meridional neutron diffraction patterns from collagen fibres in terms of the amino acid sequence. Int J Biol Macromol 2:338–346
7. Olson AJ, Bricogne G, Harrison SC (1983) Structure of tomato bushy stunt virus IV. The virus particle at 2.9 Å resolution. J Mol Biol 171:61–93
8. Koch MHJ, Stuhrmann HB (1979) Neutron scattering studies of ribosomes. Methods Enzymol 59:670–706
9. Engelman DM, Moore PB (1972) A new method for the determination of biological quaternary structure by neutron scattering. Proc Natl Acad Sci USA 69:1997–1999
10. Hoppe W (1973) The label triangulation method and the mixed isomorphous replacement principle. J Mol Biol 78:581–585
11. Moore PB, Engelman DM, Langer JA, Ramakrishnan VR, Schindler DG, Scheonborn BP, Sillers IY, Yakubi S (1984) Neutron scattering and the 30S ribosomal subunit of *E. coli*. In: Schoenborn BP (ed) Neutrons in biology. Plenum Press, New York, pp 73–91
12. May, RP, Stuhrmann HB, Nierhaus KH (1984) Structural elements of the 50S subunit of *E. coli* ribosomes. In: Schoenborn BP (ed) Neutrons in biology. Plenum Press, New York, pp. 25–45
13. Serdyuk IN, Zaccai G, Spirin AS (1978) Globular conformation of some ribosomal proteins in solution. FEBS Lett 94:349–352
14. Serdyuk IN, Shpungin JL, Zaccai G (1980) Neutron scattering study of the 13S fragment of 16S RNA and its complex with ribosomal protein S4. J Mol Biol 137:109–121
15. Moore PB, Engelman DM, Schoenborn BP (1975) A neutron scattering study of the distribution of protein and RNA in the 30S ribosomal subunit of *Escherichia coli*. J Mol Biol 91:101–120
16. Beaudry P, Petersen HU, Grunberg-Manago M, Jacrot B (1976) A neutron study of the 30S-ribosome subunit and of the 30S-IF3 complex. Biochem Biophys Res Commun 72:391
17. Ramakrishnan V (1986) Distribution of protein and RNA in the 30S ribosomal subunit. Science 231:1562–1564
18. Dessen P, Blanquet S, Zaccai G, Jacrot B (1978) Anticooperative binding of initiator transfer RNA^{Met} to methionyl-transfer RNA synthetase from *Escherichia coli*: Neutron scattering studies. J Mol Biol 126:293–313
19. Zaccai G, Jacrot B, Morin P, Moras D, Thierry JC, Giégé R (1979) Interactions of yeast valyl-tRNA synthetase with RNAs and conformational changes of the enzyme. J Mol Biol 129:483–500
20. Giégé R, Lorber B, Ebel JP, Moras D, Thierry JC, Jacrot B, Zaccai G (1982) Formation of a catalytically active complex between $tRNA^{Asp}$ and aspartyl-tRNA synthetase from yeast in high concentrations of ammonium sulphate. Biochimie 64:357–362
21. Moras D, Lorber B, Romby P, Ebel JP, Giégé R, Lewit-Bentley A, Roth M (1983) Yeast $tRNA^{Asp}$-Aspartyl-tRNA synthetase: the crystalline complex. J Biomol Struct Dynamics 1:209–223
22. Pardon JF, Cotter RI, Lilley DMJ, Worcester DL, Campbell AM, Wooley JC, Richards BM (1977) Scattering studies of chromatin subunits. Cold Spring Harbor Symp Quant Biol 42:11–22
23. Hjelm RP, Kneale GG, Suau P, Baldwin JP, Bradbury EM, Ibel K (1977) Small angle neutron scattering studies of chromatin subunits in solution. Cell 10:139–151
24. Uberbacher EC, Ramakrishnan V, Olins DE, Bunick GJ (1983) Neutron scattering studies of nucleosome structure at low ionic strength. Biochemistry 22:4916–4923
25. Finch JT, Lewit-Bentley A, Bentley GA, Roth M, Timmins PA (1980) Neutron diffraction from crystals of nucleosome core particles. Philos Trans R Soc (London) B290:635–638
26. Bentley GA, Finch JT, Lewit-Bentley A (1981) Neutron diffraction studies on crystals of nucleosome cores using contrast variation. J Mol Biol 145:771–784
27. Bentley GA, Lewit-Bentley A, Finch JT, Podjarny AD, Roth M (1984) Crystal structure of the nucleosome core particle at 16 Å resolution. J Mol Biol 176:55–76

28. Burlingame RW, Love WE, Wang B, Hamlin R, Xuong N, Mondrianakis EN (1985) Crystallographic structure of the octameric histone core of the nucleosome at a resolution of 3.3 Å. Science 228:546–553
29. Klug A, Finch JT, Richmond TJ (1985) Crystallographic structure of the octamer histone core of the nucleosome. Science 229:1109
30. Uberbacher EC, Bunick GJ (1985) Crystallographic structure of the octamer histone core of the nucleosome. Science 229:1112
31. Uberbacher EC, Harp JHM, Wilkinson-Singley E, Bunick GJ (1986) Shape analysis of the histone octamer in solution. Science 232:1247–1249
32. Abad-Zapatero C, Abdel-Meguid SS, Johnson JE, Leslie AGW, Rayment I, Rossman MG, Suck D, Tsukihara T (1980) Structure of southern bean mosaic virus at 2.8 Å resolution. Nature (London) 286:33–39
33. Jones TA, Liljas L (1984) Structure of satellite tobacco necrosis virus after crystallographic refinement at 2.5 Å resolution. J Mol Biol 177:735–767
34. Rossmann MG, Arnold E, Erickson JW, Frankenberger EA, Griffith JP, Hecht HJ, Johnson JE, Kamer G, Luo M, Mossa AG, Rueckert RR, Sherry B, Vriend G (1985) Structure of a human common cold virus and functional relationship to other picornaviruses. Nature 317:145–153
35. Hogle JM, Chow M, Filman DJ (1985) Three-dimensional structure of poliovirus at 2.9 Å resolution. Science 229: 1358–1365
36. Chauvin C, Witz J, Jacrot B (1978) Structure of the tomato bushy stunt virus: a model for protein-RNA interaction. Biol 124:641–651
37. Harrison SC (1980) Protein interfaces and intersubunit bonding. The case of tomato bushy stunt virus. Biophys J 32:139–153
38. Kruse J, Timmins PA, Witz J (1982) A neutron scattering study of the structure of compact and swollen forms of southern bean mosaic virus. Virology 119:42–50
39. Devaux C, Timmins PA, Berthet-Colominas C (1983) Structural studies of adenovirus type 2 by neutron and X-ray scattering. J Mol Biol 167:119–132
40. Cusack S (1982) Neutron scattering studies of virus structure. In: The Neutron and its applications, 1982. Inst. Phys. Conf. Ser. N°. 64, Section 4, pp 351–355
41. Cusack S (1984) Neutron scattering studies of virus structure. In: Schoenborn BP (ed) Neutrons in biology. Plenum Press, New York, pp 173–188
42. Stöckel P, May R, Strell I, Cejka Z, Hoppe W, Heumann H, Zillig W, Crespi HL, Katz JJ, Ibel K (1979) Determination of intersubunit distances and subunit shape parameters in DNA-dependent RNA polymerase by neutron small-angle scattering. J Appl Crystallogr. 12:176–185
43. Stöckel P, May R, Strell I, Cejka Z, Hoppe W, Heumann H, Zillig W, Crespi HL (1980) The core subunit structure in RNA polymerase holoenzyme determined by neutron small-angle scattering. Eur J Biochem 112:411–417
44. Stöckel P, May R, Strell I, Cejka Z, Hoppe W, Heumann H, Zillig W, Crespi HL (1980) The subunit positions within RNA polymerase holoenzyme determined by triangulation of centre-to-centre distances. Eur J Biochem 112:419–423
45. Lederer H, May R, Kjems JK, Schaeffer W, Crespi HL, Heumann H (1986) Deuterium incorporation into *Escherichia coli* proteins. A neutron scattering study of DNA-dependent RNA polymerase. Eur J Biochem 156:655–659
46. Ibel K, May RP, Kirschner K, Lane AH, Szadkowski H, Dauvergne MT, Zulauf M (1985) The domain structure of tryptophan synthase. A neutron scattering study. Eur J Biochem 151:505–514
47. Schmitt FO, Bear RS, Clark GL (1935) X-ray diffraction studies on nerve. Radiobiology 25:131–151
48. Tardieu A, Luzzati V, Reman FC (1973) Structure and polymorphism of the hydrocarbon chains of lipids: a study of lecithin/water phases. J Mol Biol 75:711–733
49. Wilkins MHF, Blaurock AE, Engelman DM (1971) Bilayer structure in membranes. Nature 230:72–76
50. Dratz EA, Hargrave PA (1983) The structure of rhodopsin and the rod outer segment disk membrane. TIBS 8:128–131
51. Saibil H, Chabre M, Worcester D (1976) Neutron diffraction studies of retinal rod outer segment membranes. Nature 262:266–270
52. Henderson R. Unwin PNT (1975) Three-dimensional model of purple membrane obtained by electron microscopy. Nature 257:2832
53. LeMaire M, Møller JV, Tanford C (1976) Retention of enzyme activity by detergent-solubilized sarcoplasmic Ca^{2+}-ATPase. Biochemistry 15:2336–2342
54. Michel H (1983) Crystallization of membrane proteins. TIBS 8:56–59
55. Deisenhofer J, Epp O, Miki K, Huber R, Michel H (1985) Structure of the protein subunits in the photosynthetic reaction centre of *Rhodopseudomonas viridis* at 3 Å resolution. Nature 318:618–624
56. Zaccai G, Blasie JK, Schoenborn BP (1975) Neutron diffration studies on the loation of water in lecithin bilayer model membranes. Proc Natl Acad Sci USA 72:376–380
57. Worcester, DL (1976) Neutron beam studies of biological membranes and membrane components. In: Chapman D, Wallach DFH (Eds) Biological membranes. Academic Press, London, pp 1–46
58. Büldt G, Seelig J (1980) Conformation of phosphatidylethanolamine in the gel phase as seen by neutron diffraction. Biochemistry 19:6170–6175
59. Büldt G, Gally HU, Seelig J, Zaccai G (1979) Neutron diffraction studies on phosphatidylcholine model membranes. I. Head group conformation. J Mol Biol 134:673–691
60. Zaccai G, Büldt G, Seelig A, Seelig J (1979) Neutron diffraction studies on phosphatidylcholine model membranes. II. Chain conformation and segmental disorder. J Mol Biol 134:693–706
61. Stoekenius W, Bogomolni RA (1982) Bacteriorhodopsin and related pigments of halobacteria. Annu Rev Biochem 52:587–616
62. Zaccai G, Gilmore D (1979) Areas of hydration in the purple membrane of *Halobacterium halobium*: A neutron diffraction study. J Mol Biol 132:181–191
63. Rogan, PK, Zaccai G (1981) Hydration in purple membrane as a function of relative humidity. J Mol Biol 145:281–283
64. Zaccai G (1987) Structure and hydration of purple membrane in different conditions. J Mol Biol 194:569–572
65. Engelman DM, Zaccai G (1980) Bacteriorhodopsin is an inside-out protein. Proc Natl Acad Sci USA 77:5894–5898
66. Trewhella J, Anderson S, Fox R, Gogol E, Khan S, Zaccai G, Engelman DM (1983) Assignment of segments of the bacteriorhodopsin sequence to positions in the structural map. Biophysics J 42:233–241
67. Popot JL, Trewhella J, Engelman DM (1986) Reformation of crystalline purple membrane from purified bacteriorhodopsin fragments. EMBO J 5:3039–3044
68. Trewhella J, Popot JL, Zaccai G, Engelman DM (1986) Localization of two chymotryptic fragments in the structure of renatured bacteriorhodopsin by neutron diffraction. EMBO J 5:3045–3049
69. Jubb JS, Worcester DL, Crespi HL, Zaccai G (1984) Retinal location in purple membrane of *Halobacterium halobium*: a neutron diffraction study of membranes labelled in vivo with deuterated retinal. EMBO J 3:1455–1461
70. Seiff F, Wallat I, Ermann P, Heyn MP (1985) A neutron diffraction study on the location of the polyene chain of

retinal in bacteriorhodopsin. Proc Natl Acad Sci USA 82:3227–3231
71. Osborne HB, Sardet C, Michel-Villaz M, Chabre M (1978) Structural study of rhodopsin in detergent micelles by small-angle neutron scattering. J Mol Biol 123:177–206
72. Peters WHM, Jansen PLH, Nanton H (1984) The molecular weights of UDP-glycuronyltransferase determined with radiation-inactivation analysis. J Biol Chem 259: 11701–11705
73. Block MR, Zaccai G, Lauquin GJM, Vignais PV (1982) Small angle neutron scattering of the mitochondrial ADP/ATP carrier protein in detergent. Biochem Biophys Res Commun 471–477
74. Zulauf M, Timmins PA, Garavito RM (1986) Neutron crystallography of a membrane protein. Localization of detergent and protein at 20-Å resolution. Biophys J 49:96–98
75. Li ZQ, Giégé R, Jacrot B, Oberthür R, Thierry JC, Zaccai G (1983) Structure of phenylalanine-accepting transfer ribonucleic acid and of its environment in aqueous solvents with different salts. Biochemistry 22:4380–4388
76. Zaccai G, Su Y-X (1987) Structure of phenylamine-accepting transfer ribonucleic acid and its environment in aqueous solvents with different salts (II). Biochemistry (in press)
77. Lehmann MS, Zaccai G (1984) Neutron small-angle scattering studies of ribonuclease in mixed aqueous solutions and determinations of the preferentially bound water. Biochemistry 23:1939–1942
78. Zaccai G (1986) Measurements of density and location of solvent associated with biomolecules by small-angle neutron scattering. Methods Enzymol 127:619–629
79. Zaccai G, Wachtel E, Eisenberg H (1986) Solution structure of halophilic malate dehydrogenase from small-angle neutron and X-ray scattering and ultracentrifugation. J Mol Biol 190:97–106
80. Zaccai G, Bunick GJ, Eisenberg H (1986) Denaturation of a halophilic enzyme monitored by small-angle neutron scattering. J Mol Biol 192:155–157
81. Jacrot B, Zaccai G (1981) Molecular weight determination by neutron scattering. Biopolymers 20:2413–2426
82. Calmettes P, Eisenberg H, Zaccai G (1987) Structure of halophilic malate dehydrogenase in multimolar KCl solutions from neutron scattering and ultracentrifugation. Biophys Chem 26:279–290
83. Middendorf D (1984) Biophysical applications of quasi-elastic and inelastic neutron scattering. Annu Rev Biophys Bioeng 13:425–452
84. Cusack S (1986) Low frequency motion in proteins and its study by inelastic neutron scattering. Comments Mol Cell Biophys 3:243–271
85. Wlodawer A (1982) Neutron diffraction of crystalline proteins. Prog Biophys Mol Biol 40:115–159
86. Braganza LF, Worcester KL (1986) Hydrostatic pressure induces hydrocarbon chain interdigitation in single-component phospholipid bilayers. Biochemistry 25:2591–2596
87. Braganza LF, Worcester DL (1986) Structural changes in lipid bilayers and biological membranes caused by hydrostatic pressure. Biochemistry 25:7484–7488
88. Eisenberg H (1981) Forward scattering of light, X-rays and neutrons. Qu Rev Biophys 14:141–172